

## Research Article

# Human Umbilical Cord MSC-Derived Exosomes Suppress the Development of CCl<sub>4</sub>-Induced Liver Injury through Antioxidant Effect

Wenqian Jiang,<sup>1</sup> Youwen Tan,<sup>2</sup> Mengjie Cai,<sup>1</sup> Ting Zhao,<sup>1</sup> Fei Mao <sup>1</sup>, Xu Zhang <sup>1</sup>,  
Wenrong Xu <sup>1,3</sup>, Zhixin Yan,<sup>1</sup> Hui Qian <sup>1,3</sup> and Yongmin Yan <sup>1</sup>

<sup>1</sup>Liver Disease and Cancer Institute, School of Medicine, Jiangsu University, Zhenjiang, Jiangsu, China

<sup>2</sup>The Affiliated Third Hospital of Zhenjiang, Jiangsu University, Zhenjiang, Jiangsu, China

<sup>3</sup>Key Laboratory of Laboratory Medicine of Jiangsu Province, School of Medicine, Jiangsu University, Zhenjiang, Jiangsu, China

Correspondence should be addressed to Hui Qian; [lstmmmlst@163.com](mailto:lstmmmlst@163.com) and Yongmin Yan; [ujjsym@163.com](mailto:ujjsym@163.com)

Received 7 August 2017; Revised 20 November 2017; Accepted 10 December 2017; Published 4 March 2018

Academic Editor: Ann Steele

Copyright © 2018 Wenqian Jiang et al. This is an open access article distributed under the Creative Commons Attribution License, which permits unrestricted use, distribution, and reproduction in any medium, provided the original work is properly cited.

Mesenchymal stem cells (MSCs) have been increasingly applied into clinical therapy. Exosomes are small (30–100 nm in diameter) membrane vesicles released by different cell types and possess the similar functions with their derived cells. Human umbilical cord MSC-derived exosomes (hucMSC-Ex) play important roles in liver repair. However, the effects and mechanisms of hucMSC-Ex on liver injury development remain elusive. Mouse models of acute and chronic liver injury and liver tumor were induced by carbon tetrachloride (CCl<sub>4</sub>) injection, followed by administration of hucMSC-Ex via the tail vein. Alleviation of liver injury by hucMSC-Ex was determined. We further explored the production of oxidative stress and apoptosis in the development of liver injury and compared the antioxidant effects of hucMSC-Ex with frequently used hepatic protectant, bifendate (DDB) in liver injury. hucMSC-Ex alleviated CCl<sub>4</sub>-induced acute liver injury and liver fibrosis and restrained the growth of liver tumors. Decreased oxidative stress and apoptosis were found in hucMSC-Ex-treated mouse models and liver cells. Compared to bifendate (DDB) treatment, hucMSC-Ex presented more distinct antioxidant and hepatoprotective effects. hucMSC-Ex may suppress CCl<sub>4</sub>-induced liver injury development via antioxidant potentials and could be a more effective antioxidant than DDB in CCl<sub>4</sub>-induced liver tumor development.

## 1. Introduction

The imbalance between oxidant and antioxidant results in oxidative stress. Most chronic liver diseases, such as alcoholic liver disease, nonalcoholic fatty liver disease, liver fibrosis, and viral hepatitis, possess the increased oxidant stress [1]. Even in the progression of hepatocarcinogenesis, oxidative stress has been recognized as a key factor and increases the possibility of hepatocarcinogenesis [2]. Although antioxidants have been regarded as a good therapeutic strategy in consideration of the importance of oxidative stress in the pathological process of liver diseases, the research findings remain inconclusive and controversial. So searching for effective methods to control the oxidative stress is still on the way.

Mesenchymal stem cells (MSCs), with multilineage differentiation potential and self-renewal ability, have given rise to interests in the potentials of repairing tissues. Increasing researches have taken advantage of MSCs to cell-based clinical trials for numerous diseases including liver diseases [3]. It is reported that MSCs exist in all tissues and can be isolated from bone marrow, adipose tissue, umbilical cord, and so on [4–6]. Human umbilical cord has been a prospective source of MSCs, with properties of proliferation and differentiation, lack of tumorigenicity, karyotype stability, and high immunomodulatory activity [7]. Our previous studies have successfully isolated the MSCs from human umbilical cord and demonstrated that human umbilical cord MSCs (hucMSCs) could ameliorate mouse hepatic injury and acute renal failure [8–11]. Early researches considered that the

therapeutic mechanism of MSCs for repairing tissues was engraftment in injured tissues and differentiation into specific cells to replace necrotic or apoptotic cells [12, 13]. Recently, studies have suggested that mechanism of MSC in tissue repair may prefer secreting soluble factors to alter the tissue microenvironment rather than differentiation solely [14].

Exosomes (30–100 nm) are small membrane-bound vesicles derived from multivesicular bodies, which can be secreted by a wide variety of cells and contain proteins, mRNAs, and noncoding RNAs as cargos being transferred to other cells [15, 16]. Exosomes derived from MSC have shown to be beneficial to neurite outgrowth, neovascularization, and renal injury [17–19]. Our previous studies demonstrated that the protective effect of hucMSC-derived exosomes (hucMSC-Ex) on tissue repair including acute renal injury (AKI), cutaneous wound, and liver fibrosis [20–22] and even illuminated that hucMSC-Ex delivered GPX1 could promote the recovery of oxidatively injured liver [23]. However, whether hucMSC-Ex have any effects on liver injury development is not clear.

Bifendate, a synthetic intermediate of schisandrin C, was found to protect against drug-induced liver injury in animals and is now used clinically for the treatment of hepatitis [24]. In this study, we investigated the effects of hucMSC-Ex on liver injury development and explored the underlying mechanism preliminarily. We demonstrated that hucMSC-Ex could suppress CCl<sub>4</sub>-induced acute and chronic liver injury and liver tumor growth in mice. Furthermore, we compared the antioxidative and antiapoptotic effects of hucMSC-Ex with that of bifendate (DDB) in CCl<sub>4</sub>-induced acute liver injury.

## 2. Materials and Methods

**2.1. Cell Culture.** Fresh umbilical cords were harvested from informed, consenting mothers and processed within 6 h according to the experiment protocols approved by Jiangsu University (2012258) as previously described [8]. hucMSCs were cultured in L-DMEM containing 10% fetal bovine serum (FBS) (Bovogen, Australia) at 37°C with 5% CO<sub>2</sub>. Human normal hepatic L02 cells (Chinese Academy of Science) were maintained in RPMI 1640 containing 10% FBS (Bovogen, Australia) at 37°C with 5% CO<sub>2</sub>.

**2.2. Isolation and Characterization of Exosomes.** Exosomes were isolated and purified as described previously [25]. Cell-conditioned medium with 10% FBS in which bovine exosomes and protein aggregates were removed by ultracentrifugation at 10000 ×g for 16 h at 4°C. Following 48 h culture, cell supernatants were collected and centrifuged at 2000 ×g for 20 min to remove cell debris and then centrifuged at 1000 ×g for 30 min using a 100 kDa molecular weight cutoff ultrafiltration membrane (MWCO) (Millipore, Billerica, Massachusetts, USA) to concentrate. After that, the concentrated supernatants were loaded upon a 30% sucrose/D<sub>2</sub>O cushion and ultracentrifuged at 100000 ×g for 2 h at 4°C. Exosomes were gathered from the bottom of the tube and washed with PBS for three times by centrifugation at

1000 ×g for 30 min using a 100 kDa MWCO (Millipore, Billerica, Massachusetts, USA). Exosomes were finally filtrated on a 0.22 μm pore filter (Millipore, Billerica, Massachusetts, USA) and stored at –80°C. Concentration of concentrated exosomes was determined by nanoparticle tracking analysis (NTA) (NanoSight, Amesbury, U.K.). Exosomes were also identified by transmission electron microscopy (FEI Tecnai 12, Philips, Netherlands) for the morphology and the size and ImageStreamX Imaging Flow Cytometer (Amnis, WA, USA) for exosomal markers, CD9 and CD63.

**2.2.1. Animal Model and Exosome Injection.** BALB/c female mice aged 4–5 weeks were purchased from the Laboratory Animal Center (Yangzhou University, China), and all experiment procedures were in accordance with the Chinese legislation regarding experiment animals. All the models were induced by intraperitoneal injection with 10% CCl<sub>4</sub> dissolved in mineral oil, and the final dose was 0.3 ml CCl<sub>4</sub>/kg body weight. The normal group without any treatment was used as control ( $n = 6$ ). Mice with liver tumor were induced with CCl<sub>4</sub> every 3 days for 8 months and then treated with PBS ( $n = 6$ ) or hucMSC-Ex ( $n = 6$ ) via the tail vein. At 1 month after treatment, livers were harvested from sacrificed mice for further analysis. Mice for establishing liver fibrosis were treated with CCl<sub>4</sub> every 3 days for 5 months and randomized into 2 groups for treating with PBS ( $n = 10$ ) or hucMSC-Ex ( $n = 10$ ). The dose of hucMSC-Ex was  $6.4 \times 10^9$  particles per mouse diluted in 330 μl PBS. One month later, mice were sacrificed to collect livers. Mice for acute liver injury were injected with CCl<sub>4</sub> twice for an interval of 3 days. For the analysis of hucMSC-Ex in acute liver injury, mice were randomized into 2 groups for treating with PBS ( $n = 10$ ) or hucMSC-Ex ( $6 \times 10^{10}$  particles/kg;  $n = 10$ ) by tail vein administration. For the comparison of antioxidative ability between hucMSC-Ex and DDB, mice were randomized into 2 groups for treating with hucMSC-Ex or DDB by intragastric administration at 24 h post-CCl<sub>4</sub> injection. In each group, mice were divided into 3 groups randomly with the doses of hucMSC-Ex at  $6 \times 10^{10}$  particles/kg ( $n = 10$ ),  $1.2 \times 10^{11}$  particles/kg ( $n = 10$ ), and  $2.4 \times 10^{11}$  particles/kg ( $n = 10$ ) or DDB at 8 mg/kg ( $n = 10$ ), 16 mg/kg ( $n = 10$ ), and 32 mg/kg ( $n = 10$ ). At another 24 h, mice were sacrificed for further analysis.

**2.3. CCl<sub>4</sub>-Induced L02 Cell Injury In Vitro.** L02 cells were seeded in six-well plates at  $1 \times 10^5$  cells/well and were cultured with medium containing 0.1 mM CCl<sub>4</sub>/hucMSC-Ex (0 particles/ml,  $4 \times 10^8$  particles/ml, and  $16 \times 10^8$  particles/ml) for 24 hr. After hucMSC-Ex treatment, L02 cells were collected for further detection.

**2.4. Exosome Labeling and Tracing in Mice.** According to the manufacturer's instructions, exosomes were incubated with the cross-linkable membrane dye, CM-DiR (Ruitai bio, Beijing, China), for 30 min at 37°C in the dark. After washing with PBS, the labeled exosomes were concentrated with a 100 kDa MWCO (Millipore, Billerica, Massachusetts, USA) at 1000 ×g for 30 min at 4°C to remove nonbinding dye.

TABLE 1: Primers for real-time RT-PCR.

Genes	Primer sequence (5'-3')	Annealing temperature (°C)	Product size (bp)
Mouse collagen I	For: TGAGACAGGCGAACAAGGTG	63	320
	Rev: GCTGAGGCAGGAAGCTGAAG		
Mouse collagen III	For: CTGGTCAGCCTGGAGATAAG	58	284
	Rev: ACCAGGACTACCACGTTTAC		
$\beta$ -Actin	For: CACGAAACTACCTTCAACTCC	58	265
	Rev: CATACTCCTGCTTGCTGATC		

Then CM-DiR-labeled exosomes were injected into CCl<sub>4</sub>-induced mice via the tail vein. After injection for 24 h, mice were imaged using a Maestro in Vivo Imaging System (CRI) to observe the distribution of exosomes.

**2.5. Histopathological Staining.** Liver tissues were fixed in 4% formaldehyde solution at room temperature overnight, embedded in paraffin, and cut into 4  $\mu$ m sections. The sections were stained with hematoxylin and eosin, Sirius red (Yeasen Biotechnology, Shanghai, China), and Masson trichrome (MT) (Gefan Biotechnology, Shanghai, China) in accordance with standard protocols. To analyze the extent of liver fibrosis, randomly picked fields of MT sections were captured from each animal.

**2.6. Immunohistochemistry.** Following deparaffinization and rehydration, the liver slides were steamed in citrate buffer (10 mM, pH 6.0) for 30 min for antigen retrieval and exposed to 3% hydrogen peroxide for 30 min for inhibiting endogenous peroxidase activity. Slides were then blocked in 5% bovine serum albumin for 1 h and incubated with the primary antibodies against SOX9 (Santa Cruz, Dallas, Texas, USA), 8-OHdG (Japan Institute for control of aging), activated caspase 3, Bax, and PCNA (both were from Bioworld, Louis Park, Minnesota, USA) overnight and then incubated with secondary antibody for 30 min at 37°C. Finally, slides were visualized with 3,3'-diaminobenzidine and counterstained with hematoxylin for microscopy examination (200 $\times$ ).

**2.7. Western Blotting.** hucMSC-Ex were lysed in RIPA buffer. Equal amount of protein was loaded and separated on a 12% SDS-PAGE gel. After electrophoresis, protein was transferred to PVDF membranes. The transferred membranes were blocked in 5% (w/v) skim milk for 1 h and incubated with the primary antibodies against CD9, CD63, Bcl2 (both were from Bioworld, Louis Park, Minnesota, USA), cleaved Casp3 (Santa Cruz, TX, USA), and GAPDH (KangCheng, Shanghai, China) at 4°C overnight and then incubated with HRP-conjugated goat anti-rabbit antibody for 1 h at 37°C. The signals were detected with a luminata™ crescendo Western HRP substrate (Millipore, Billerica, Massachusetts, USA) quantitated by a Molecular Dynamic Densitometer (Sage Creation Science) with LANE 1D software.

**2.8. Lipid Peroxidation MDA Assay.** Liver tissues were thawed on ice and then grinded into homogenate. Prepared homogenate was centrifuged at 400  $\times$ g for 15 min to remove

debris. The supernatant was then collected to measure MDA according to the manufacturer's instructions (Beyotime, Shanghai, China) and total protein concentration with a BCA assay kit (CW BIO, Beijing, China). MDA levels were normalized to milligrams of protein.

**2.9. ELISA Assay.** TGF- $\beta$  levels in fibrotic liver tissues treated with PBS or hucMSC-Ex were determined using an ELISA kit (Boster, Wuhan, China) according to the manufacturer's instructions.

**2.10. TUNEL Assay.** The apoptotic cells in liver slides were measured by using an in situ cell apoptosis kit (Vazyme, Nanjing, China) according to the manufacturer's instructions.

**2.11. Real-Time RT-PCR.** Total RNA of mouse livers was extracted with the Trizol reagent according to the manufacturer's instructions (Invitrogen, Shanghai, China). The cDNA was synthesized using Super Script™ RT kit according to the manufacturer's instructions (Invitrogen, Shanghai, China). The sequences of primers are shown in Table 1.

**2.12. ROS Measurement.** Cellular reactive oxygen species (ROS) of L02 cells was measured with a 2'-7'-dichlorofluorescein diacetate (DCF-DA) (Beyotime, Nantong, China) staining according to the instruction. Percentage and fluorescence intensity of DCF-positive cells were detected with the ImageStreamX Imaging Flow Cytometer (Amnis Corporation, Seattle, WA) and Olympus Fluorescent Microscope, respectively [23].

**2.13. Statistical Analysis.** Data are expressed as the means  $\pm$  standard deviation (SD). Statistical significance was assessed by Student's *t*-test (two-tailed) using Prism software (GraphPad, San Diego, USA). *P* value < 0.05 was considered significant.

### 3. Results

**3.1. hucMSC-Ex Suppressed the Development of Liver Tumor.** To characterize hucMSC-Ex, primary hucMSCs were cultured in exosome-free media (Figure 1(a)). The exosomes were isolated and subjected to biochemical and biophysical analyses. Analysis of exosomes by transmission electron microscopy revealed that hucMSC-Ex were spheroid morphology with the diameter of 30–100 nm (Figure 1(b)). Imaging flow cytometry and Western blot analysis of

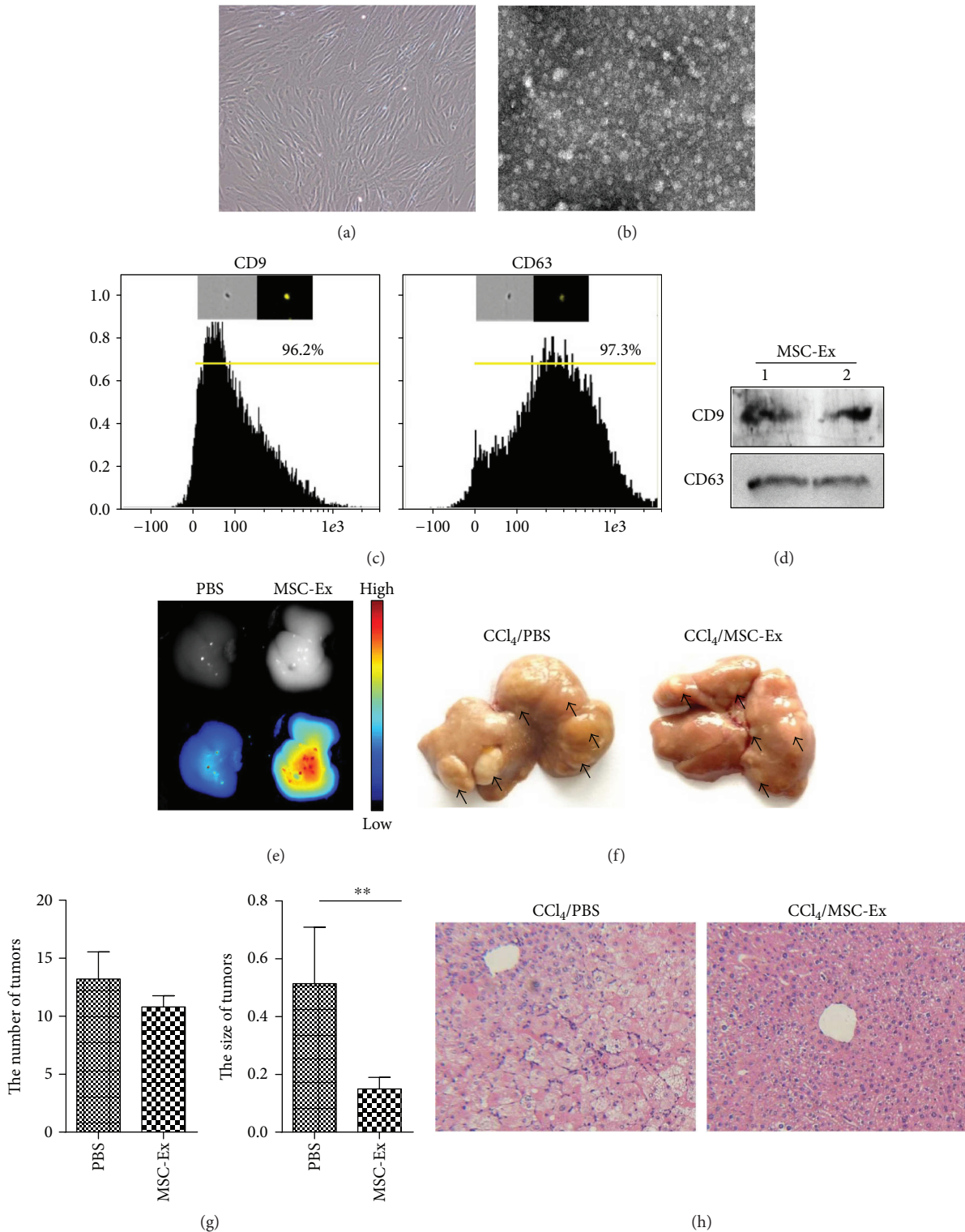


FIGURE 1: hucMSC-Ex suppressed CCl<sub>4</sub>-induced mouse liver tumor growth. (a) Morphological appearance of cultured hucMSCs. Original magnification 200x. (b) Identification of hucMSC-Ex with transmission electron micrograph. Scale bar 100 nm. (c) Imaging flow cytometer analysis of phenotypic markers of hucMSC-Ex. hucMSC-Ex were positive for CD9 and CD63. (d) Western blot assay indicated the positive expression of CD9 and CD63 proteins in hucMSC-Ex. (e) Distribution of CM-DiR labeled hucMSC-Ex in CCl<sub>4</sub>-induced hepatic carcinoma mice by in vivo fluorescent imaging. (f) Macroscopical observation of tumors in the liver surface of mice treated with PBS or hucMSC-Ex. The arrows indicated the tumors. (g) Analysis of the number and average size of tumors in the livers. Tumor size was significantly reduced in the hucMSC-Ex group ( $n = 6$ ;  $**P < 0.01$ ). (h) Representative images of H&E staining in the livers treated with PBS or hucMSC-Ex. Original magnification 100x.

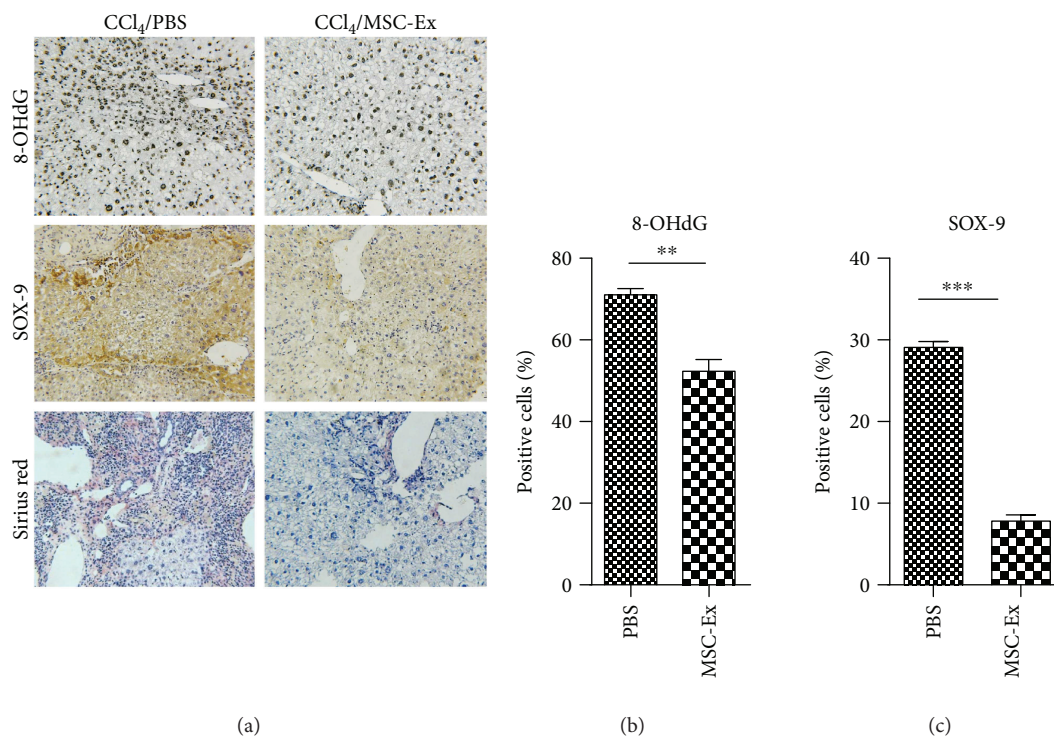


FIGURE 2: hucMSC-Ex reduced oxidative stress in mouse liver tumor. (a, b) The levels of 8-OHdG, SOX9, and collagen in mouse livers were measured by immunohistochemistry or Sirius red staining in liver tumor treated with PBS or hucMSC-Ex. Original magnification 200x. Compared with the PBS group, hucMSC-Ex significantly reduced production of oxidative stress marker 8-OHdG, SOX9 expression, and collagen deposition in liver tumor ( $n = 6$ ;  $**P < 0.01$ ,  $***P < 0.001$ ).

exosomes demonstrated expression of the exosomal proteins CD9 and CD63 (Figures 1(c) and 1(d)).

To determine if hucMSC-Ex had any restrain effect on the development of liver tumor, CCl<sub>4</sub>-induced mouse liver tumor models were established and hucMSC-Ex was infused into the mouse intravenously. In vivo fluorescent imaging showed that CM-DiR labeled hucMSC-Ex mainly located at the liver at 24 h postinjection (Figure 1(e)). After treatment with CCl<sub>4</sub> for 8 months, tumors were found on the surface of the livers. There is no difference in the number of liver tumors between the PBS group and the hucMSC-Ex group (Figure 1(f)). However, the size of tumors was obviously decreased in the hucMSC-Ex group compared with that in the PBS group (Figure 1(g);  $**P < 0.01$ ). Hematoxylin and eosin (H&E) staining confirmed reduced areas of inflammation infiltration after hucMSC-Ex treatment (Figure 1(h)). These findings suggested that hucMSC-Ex could suppress the growth of liver tumor.

### 3.2. hucMSC-Ex Inhibited Oxidative Stress in Liver Tumor.

Oxidative stress plays an essential role in the development of liver tumor. The hepatotoxicity of CCl<sub>4</sub> is mainly about oxidative damage mediated by the production of reactive free radicals and results in damage to cells. To determine if there was any effect of hucMSC-Ex on liver tumor, the levels of oxidative stress product 8-OHdG were detected in the mice of the PBS or hucMSC-Ex group. Compared with the PBS group, 8-OHdG reduced significantly in the hucMSC-Ex group (Figures 2(a) and 2(b)). SOX9, an SRY-related HMG

box transcription factor, is a progenitor/precursor cell marker of the liver expressed during embryogenesis, liver injury, and liver tumor [26]. Simultaneously, results of immunohistochemistry showed that SOX9 was downregulated in hucMSC-Ex treated mice (Figures 2(a) and 2(c)). Collagen deposition was also inhibited in the hucMSC-Ex group compared to the PBS group (Figure 2(a)). Thus, we preliminarily considered that hucMSC-Ex could reduce oxidative stress levels in liver tumor.

### 3.3. hucMSC-Ex Reduced Oxidative Stress and Inhibited Apoptosis in Liver Fibrosis.

Liver tumors develop in the context of chronic liver diseases such as CCl<sub>4</sub>-induced liver fibrosis. We then investigated the effects of hucMSC-Ex on CCl<sub>4</sub>-induced mouse liver fibrosis. To illustrate the antifibrotic effect, mice suffering liver fibrosis were handled with hucMSC-Ex, and PBS was used as controls. H&E staining showed that hucMSC-Ex treatment inhibited infiltration of inflammatory cells, hepatocyte apoptosis, and lobule destruction compared to PBS controls (Figure 3(a)). In the hucMSC-Ex group, obviously decreased areas of blue or green matrix which indicates collagen deposition were observed (Figure 3(a)). Moreover, the expression of collagen I and III detected by real-time RT-PCR decreased remarkably after hucMSC-Ex transplantation (Figure 3(b);  $*P < 0.05$ ,  $**P < 0.01$ ).

To confirm the abilities of hucMSC-Ex against oxidative stress and apoptosis in liver fibrosis, 8-OHdG and activated caspase 3 were detected by immunohistochemistry.

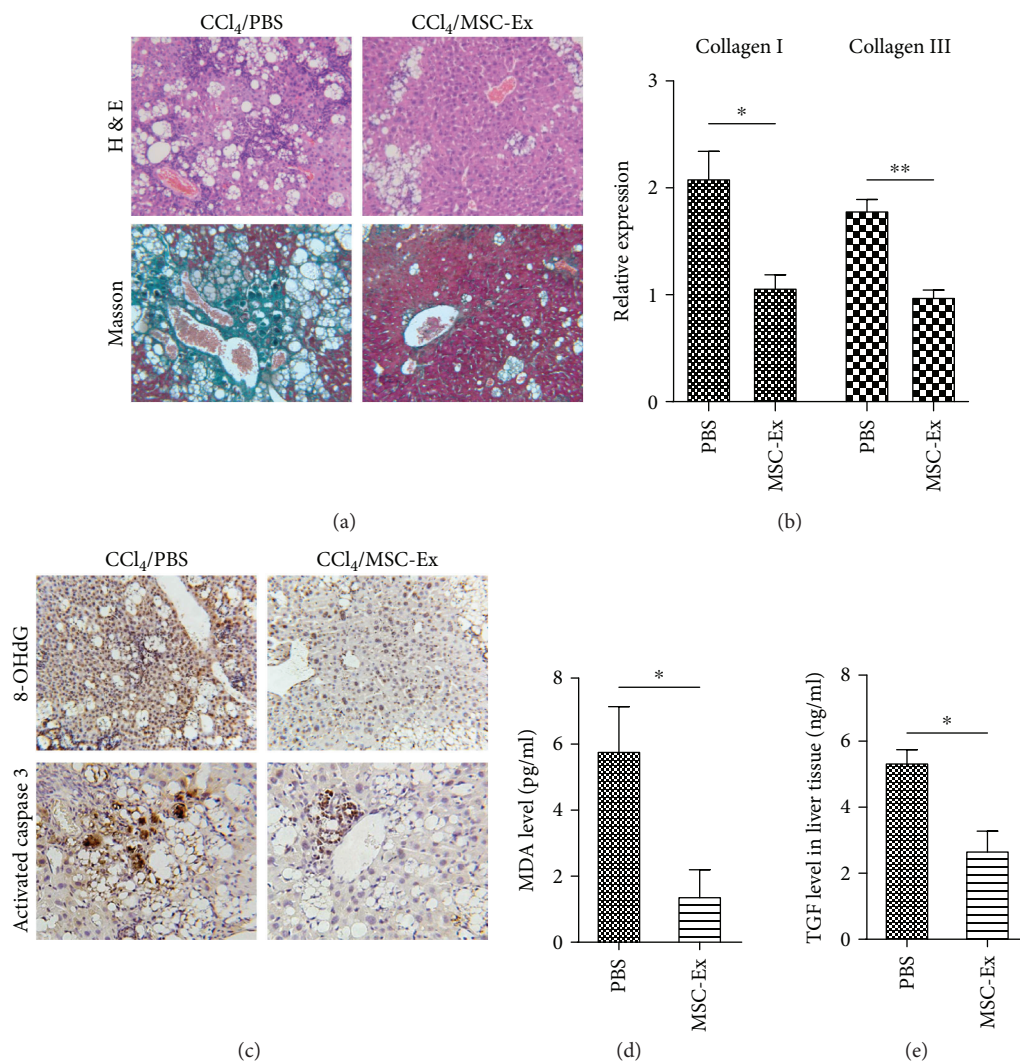


FIGURE 3: hucMSC-Ex reduced oxidative stress in mouse liver fibrosis. (a) Representative images of H&E and Masson staining of mouse fibrotic livers after PBS or hucMSC-Ex treatment. Reduced steatosis and collagen deposition were observed in the hucMSC-Ex group. Original magnification 200x. (b) Quantitative analyses of collagen I and III mRNA expression after hucMSC-Ex treatment ( $n = 10$ ;  $*P < 0.05$ ,  $**P < 0.01$ ). (c) Immunohistochemistry analysis of 8-OHdG and activated caspase 3 after administration of PBS or hucMSC-Ex. Original magnification 200x. (d, e) MDA and TGF- $\beta$  levels were measured in homogenates of a mouse fibrotic liver treated with PBS and hucMSC-Ex. The levels of MDA and TGF- $\beta$  were inhibited by hucMSC-Ex compared with the PBS group ( $n = 10$ ;  $*P < 0.05$ ).

Compared to PBS, hucMSC-Ex significantly inhibited activated caspase 3 and 8-OHdG production in mouse liver fibrosis models (Figure 3(c)). The levels of MDA and TGF- $\beta$  in livers were also reduced in the hucMSC-Ex group (Figures 3(d) and 3(e);  $*P < 0.05$ ). Thus, hucMSC-Ex may have potentials of oxidation resistance and antiapoptosis in liver fibrosis.

**3.4. hucMSC-Ex Reduced Oxidative Stress and Inhibited Apoptosis in Acute Liver Injury.** To further assess the antioxidative and antiapoptotic effects of hucMSC-Ex, they were injected intravenously into mouse models with acute liver injury induced by CCl<sub>4</sub>. The decrease of 8-OHdG production in an injured liver was found at 24 h after treatment with hucMSC-Ex (Figures 4(a) and 4(b);  $*P < 0.05$ ,  $***P < 0.001$ ). Activated caspase 3 and BAX have been shown to be involved in cell apoptosis. Then we explored

the expression of activated caspase 3 and BAX. Results of Bax and activated caspase 3 staining showed cell apoptosis-associated gene expression was decreased after hucMSC-Ex treatment (Figures 4(a)–4(c);  $*P < 0.05$ ,  $***P < 0.001$ ). TUNEL staining also revealed that hucMSC-Ex treatment could inhibit the apoptosis in liver injury (Figures 4(c) and 4(d);  $***P < 0.001$ ). Therefore, hucMSC-Ex can reverse oxidative stress-induced apoptosis in CCl<sub>4</sub>-induced acute liver injury.

**3.5. Comparison of Antioxidative Ability between hucMSC-Ex and DDB in Acute Liver Injury.** Bifendate (DDB) is frequently used in clinical therapy and can alleviate liver damage induced by CCl<sub>4</sub>. To identify the antioxidant ability of hucMSC-Ex, different doses of hucMSC-Ex ( $6 \times 10^{10}$  particles/kg,  $1.2 \times 10^{11}$  particles/kg, and  $2.4 \times 10^{11}$  particles/kg) and DDB (8 mg/kg, 16 mg/kg, and 32 mg/kg) were given

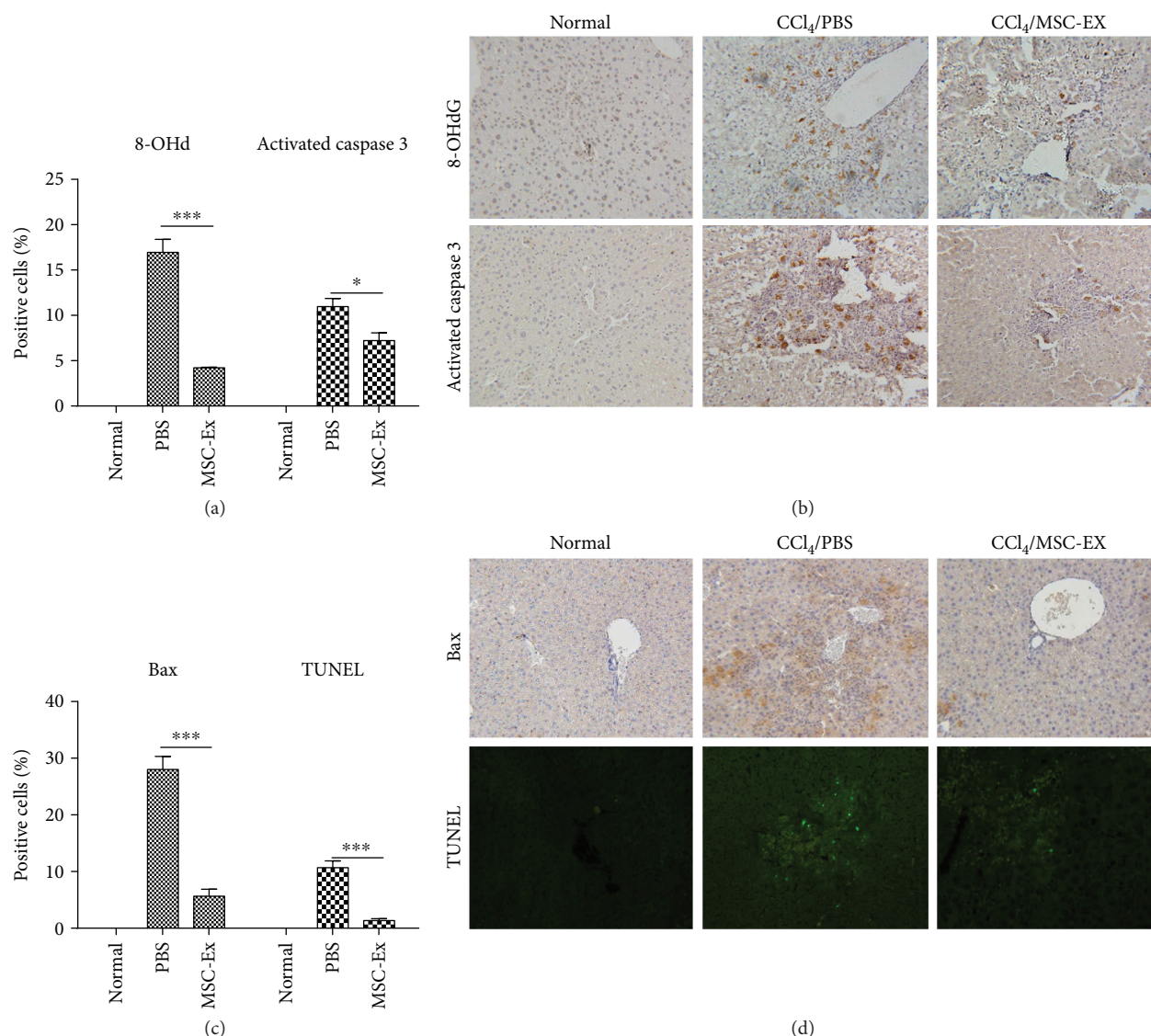


FIGURE 4: hucMSC-Ex reduced oxidative stress in acute liver injury. (a, b) Immunohistochemistry staining of 8-OHdG and activated caspase 3 in mouse livers. Reduced production of oxidative stress marker 8-OHdG and activated caspase 3 expression was detected in the hucMSC-Ex group ( $n = 10$ ;  $*P < 0.05$ ,  $***P < 0.001$ ). Original magnification 200x. (c, d) Immunohistochemistry staining of Bax and TUNEL in mouse liver slides. Bax expression and cell apoptosis were decreased in the hucMSC-Ex group ( $n = 10$ ;  $***P < 0.001$ ). Original magnification 200x.

24 h after administration of  $\text{CCl}_4$ . We observed more integrated hepatic tissue structure and less hepatic lobule destruction in the hucMSC-Ex group at  $1.2 \times 10^{11}$  particles/kg compared with the DDB group at 16 mg/kg. Expression of 8-OHdG and activated caspase 3 was dose-dependently decreased in both the hucMSC-Ex group and the DDB group (Figures 5(a)–5(d);  $*P < 0.05$ ,  $**P < 0.01$ , and  $***P < 0.001$ ). Compared with the PBS group, hucMSC-Ex ( $2.4 \times 10^{11}$  particles/kg) exerted a more distinct inhibition effect on the expression of 8-OHdG and activated caspase 3 (Figures 5(a)–5(d);  $*P < 0.05$ ,  $**P < 0.01$ , and  $***P < 0.001$ ).

To further analyze the antioxidative effects of hucMSC-Ex *in vitro*, ROS level of the L02 cells were detected by using a DCF-DA probe. Results of imaging flow cytometry and fluorescence microscope showed that the percentage and fluorescence intensity of DCF-positive hepatocytes

decreased after hucMSC-Ex treatment (Figures 6(a)–6(c);  $***P < 0.001$ ). hucMSC-Ex treatment also promoted the expression of proliferating cell nuclear antigen (PCNA) (Figure 6(d)) and inhibited cell apoptosis-associated activated caspase 3 expression (Figure 6(e)). These findings demonstrated that hucMSC-Ex could be an effective antioxidant in  $\text{CCl}_4$ -induced injury (Figure 6(f)).

#### 4. Discussion

The capacities of MSCs including differentiation, immunomodulation, and bioactive molecule release determine the potentials to treat organ diseases induced by tissue injury or degeneration. A series of clinical trials was performed on patients with diseases such as liver cirrhosis and acute-on-chronic liver failure, which have demonstrated that hucMSC

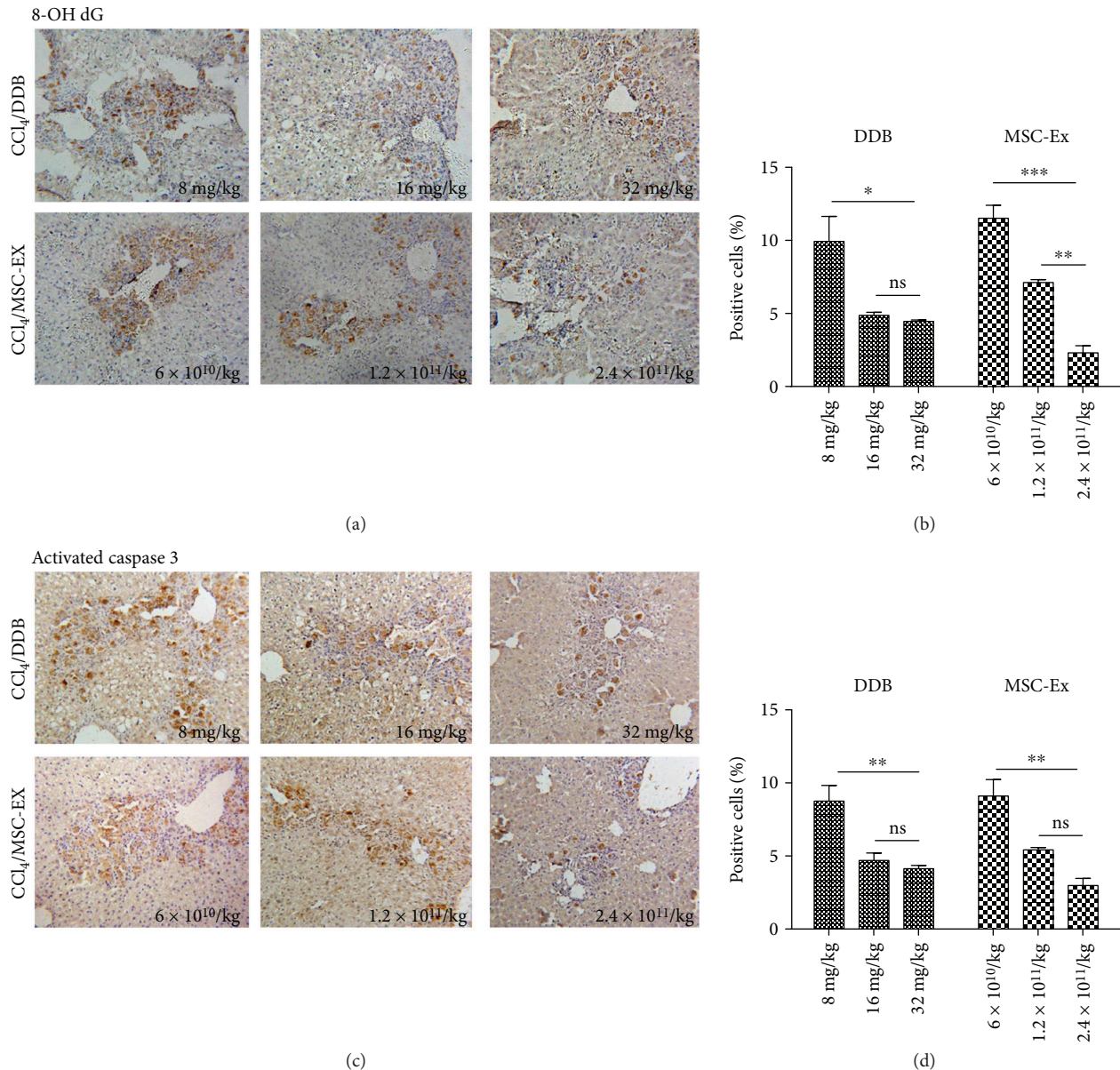


FIGURE 5: hucMSC-Ex exerted a more effective antioxidant than DDB in CCl<sub>4</sub>-induced liver injury. (a, b) Immunohistochemistry staining of 8-OHdG in mouse livers after treatment with DDB (8 mg/kg, 16 mg/kg, and 32 mg/kg) or hucMSC-Ex ( $6 \times 10^{10}$  particles/kg,  $1.2 \times 10^{11}$  particles/kg, and  $2.4 \times 10^{11}$  particles/kg) ( $n = 10$ ; \* $P < 0.05$ , \*\* $P < 0.01$ , and \*\*\* $P < 0.001$ ). (c, d) Immunohistochemistry staining of activated caspase 3 in mouse livers after treatment with DDB (8 mg/kg, 16 mg/kg, and 32 mg/kg) or hucMSC-Ex ( $6 \times 10^{10}$  particles/kg,  $1.2 \times 10^{11}$  particles/kg, and  $2.4 \times 10^{11}$  particles/kg) ( $n = 10$ ; \*\* $P < 0.01$ ). Compared with the PBS group, hucMSC-Ex ( $2.4 \times 10^{11}$  particles/kg) exerted a more distinct inhibition effect in the expression of 8-OHdG and activated caspase 3. Original magnification 200x.

improved liver function and increased survival rates [27, 28]. Increasing evidences have demonstrated the paracrine effects of MSC on tissue repair; for example, Zhang et al. suggested that hucMSC rescue acute liver failure via paracrine actions to promote liver regeneration but not primarily attributing to differentiation into hepatocytes [29]. hucMSC-Ex consisting in hucMSC-conditioned medium contain proteins, mRNAs, noncoding RNAs, and other elements derived from the cells. Moreover, it has been reported that human MSC transplantation may promote tumor growth, while exosomes derived from hucMSC are supposed to be relatively safe [30, 31]. Given the similar functions of

exosomes and their derived MSCs, it should be crucial for hucMSC-Ex on liver injury repair, simultaneously according to our previous studies [20, 32]. Even so, there is still no evidence stating any effect on liver injury development of hucMSC-Ex. Therefore, the present study was performed to illustrate the hepatoprotective role of hucMSC-Ex against liver injury development.

CCl<sub>4</sub> is a hepatotoxic chemical and is frequently used to induce liver injury. After 8-month injection of CCl<sub>4</sub>, we successfully established a mouse model of liver tumor. Our data showed that after administration of hucMSC, the average volume of liver tumors was distinctly diminished. Although



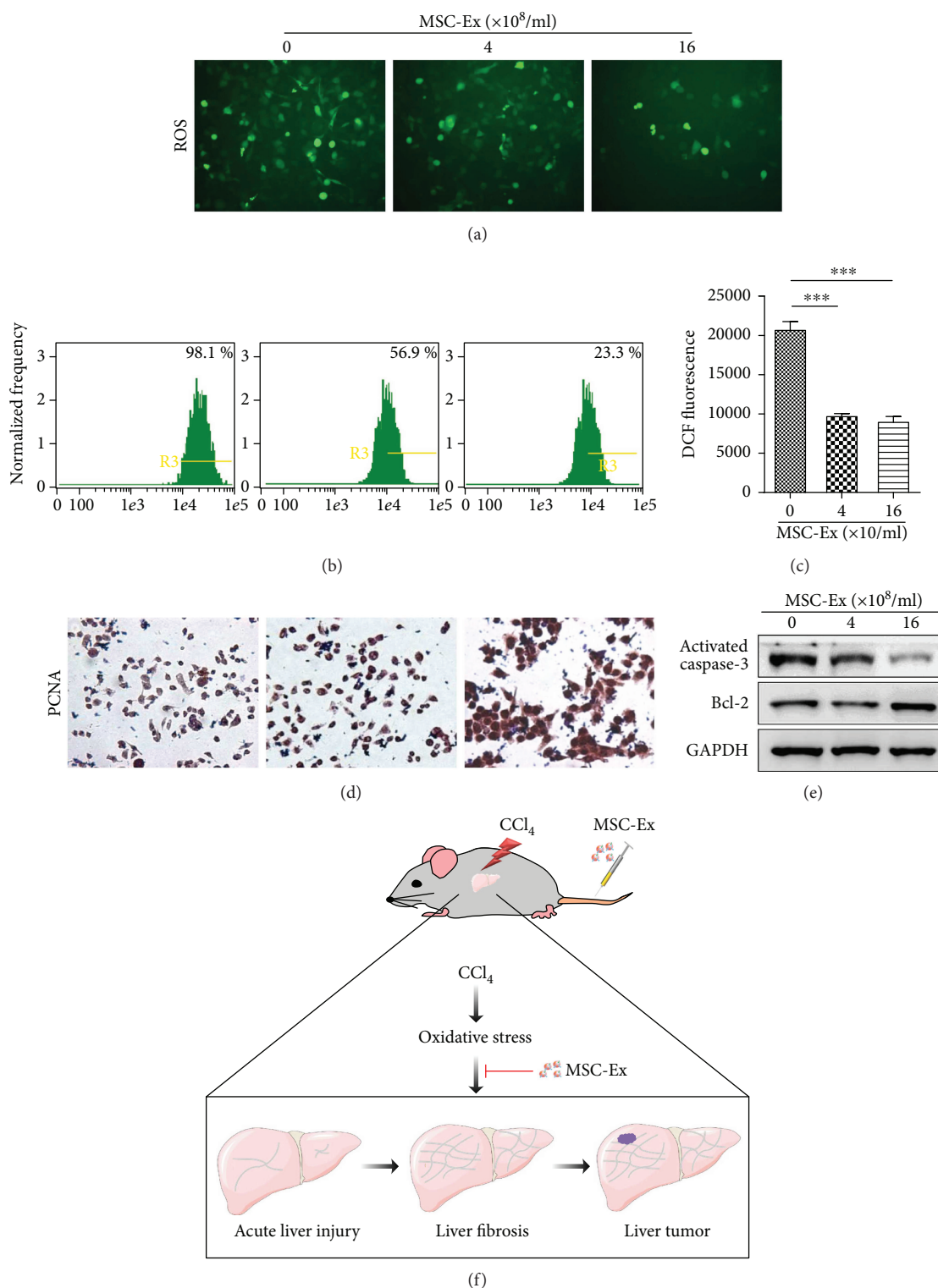


FIGURE 6: hucMSC-Ex inhibits oxidative stress in CCl<sub>4</sub>-injured L02 cells. (a) ROS production in CCl<sub>4</sub>-injured L02 cells treated with different doses of hucMSC-Ex (0 particles/ml, 4 × 10<sup>8</sup> particles/ml, and 16 × 10<sup>8</sup> particles/ml). Original magnification 200x. (b) Percentage of DCF-positive hepatocytes in hucMSC-Ex treated L02 cells using imaging flow cytometer. Data showed that hucMSC-Ex significantly decreased percentage of DCF-positive hepatocytes. (c) Fluorescence intensity of DCF-positive L02 cells was significantly decreased by hucMSC-Ex treatment. DCF fluorescent values are means ± SD. (n = 3; \*\*\*P < 0.001). (d) Immunohistochemistry staining of PCNA in hucMSC-Ex-treated L02 cells. Percentage of PCNA-positive L02 cells and PCNA expression was enhanced in the hucMSC-Ex group compared with that in the PBS group. Original magnification 200x. (e) Western blot quantification of activated caspase 3 and Bcl2. hucMSC-Ex induced Bcl2 expression and inhibited activated caspase 3 expression in CCl<sub>4</sub>-injured L02 cells. (f) Experimental model design of hucMSC-Ex in CCl<sub>4</sub>-induced liver tumor development.

doses of 250  $\mu\text{g}$  exosomes were enough to ameliorate liver fibrosis and 200  $\mu\text{g}$  exosomes to improve wound healing, we still chose the high dose of hucMSC-Ex to transplant to observe the tumor-suppressive function with the consideration of severity of injured tissues in liver tumor.

Approximately 90% of liver tumors were developed in liver cirrhosis accompanied with chronic inflammation in which oxidative stress plays an influential role [33]. So far, oxidative stress has been the explanation of numerous liver disorders, and hence, we inferred that hucMSC-Ex exert tumor-suppressive function via inhibiting oxidative stress. Liver fibrosis, characterized by hepatic stellate cell activation and overdeposition of extracellular matrix, is the inevitable stage in the development of liver cirrhosis. Oxidative stress can also induce hepatic apoptosis [34]. We measured the high levels of 8-OHdG, activated caspase 3, and MDA in fibrotic livers, and hucMSC-Ex, as was expected, reduced the expression of these proteins. hucMSC-Ex also decreased TGF- $\beta$  levels which are always induced in damaged livers and trigger hepatocyte destruction and hepatic stellate activation [35]. With regard to inflammation, hucMSC increased anti-inflammatory cytokines with the passage of time meanwhile it decreased proinflammatory cytokines, which indicated the relief of inflammatory reaction. Similar findings were observed in acute liver injury in vivo and in vitro that hucMSC-Ex exerted capacities of oxidation resistance and antiapoptosis. Wang had proved that exosomes derived from MSC gave play to hepatoprotective effects via activation of proliferation and regeneration [36]. In in vitro experiment, hucMSC-Ex presented obvious auxoaction of hepatocyte proliferation.

In spite of our understanding about the hepatoprotective effects of hucMSC-Ex, we still did not know well these potencies compared with other medicines. As is known to all, DDB, a synthetic intermediate of schisandrin C, is used to treat hepatitis with minimal side effects and is always regarded as positive control when exploring hepatoprotective actions [37, 38]. In the present study, we found that DDB presented the oxidation resistance and antiapoptotic potential with the increase of using dosage as well as hucMSC-Ex. However, there remained differences between the groups and the hepatoprotective effects of hucMSC-Ex were presented more distinctly than DDB.

In conclusion, we unraveled that hucMSC-Ex presented hepatoprotective activities through antioxidant defenses in the disease progression from initial liver injury to fibrosis and even to liver tumor. During the pathogenesis and regression of liver diseases, nevertheless, there are multifarious hepatotropic networks concerning tissue regulation and homeostasis [39], and hence, it is necessary to explore the further mechanism how hucMSC-Ex exert antioxidant activities in liver injury development.

## 5. Conclusions

hucMSC-Ex may suppress liver injury development via antioxidant potentials and could be a more effective antioxidant than DDB in liver injury.

## Conflicts of Interest

The authors declare no conflict of interest.

## Authors' Contributions

Wenqian Jiang and Youwen Tan contributed equally to this work.

## Acknowledgments

This work was funded by the National Natural Science Foundation of China (Grant nos. 81670549, 81200312, and 81641174), China Postdoctoral Science Foundation (2015M580403, 2016T90431), Natural Science Foundation of Jiangsu Province (Grant no. BE2016717), the Scientific Research Foundation of Jiangsu University (Grant no. 11JDG062), Priority Academic Program Development of Jiangsu Higher Education Institutions (PAPD), and Young Backbone Teacher Training Project of Jiangsu University.

## References

- [1] H. Cichoż-Lach and A. Michalak, "Oxidative stress as a crucial factor in liver diseases," *World Journal of Gastroenterology*, vol. 20, no. 25, pp. 8082–8091, 2014.
- [2] A. Takaki and K. Yamamoto, "Control of oxidative stress in hepatocellular carcinoma: helpful or harmful?," *World Journal of Hepatology*, vol. 7, no. 7, pp. 968–979, 2015.
- [3] T. Squillaro, G. Peluso, and U. Galderisi, "Clinical trials with mesenchymal stem cells: an update," *Cell Transplantation*, vol. 25, no. 5, pp. 829–848, 2016.
- [4] F. Anjos-Afonso and D. Bonnet, "Nonhematopoietic/endothelial SSEA-1<sup>+</sup> cells define the most primitive progenitors in the adult murine bone marrow mesenchymal compartment," *Blood*, vol. 109, no. 3, pp. 1298–1306, 2007.
- [5] P. S. In 't Anker, S. A. Scherjon, C. Kleijburg-van der Keur et al., "Isolation of mesenchymal stem cells of fetal or maternal origin from human placenta," *Stem Cells*, vol. 22, no. 7, pp. 1338–1345, 2004.
- [6] P. A. Zuk, M. Zhu, H. Mizuno et al., "Multilineage cells from human adipose tissue: implications for cell-based therapies," *Tissue Engineering*, vol. 7, no. 2, pp. 211–228, 2001.
- [7] I. Arutyunyan, A. Elchaninov, A. Makarov, and T. Fatkhudinov, "Umbilical cord as prospective source for mesenchymal stem cell-based therapy," *Stem Cells International*, vol. 2016, Article ID 6901286, 17 pages, 2016.
- [8] C. Qiao, W. Xu, J. H. W. Zhu et al., "Human mesenchymal stem cells isolated from the umbilical cord," *Cell Biology International*, vol. 32, no. 1, pp. 8–15, 2008.
- [9] Y. Yan, W. Xu, H. Qian et al., "Mesenchymal stem cells from human umbilical cords ameliorate mouse hepatic injury in vivo," *Liver International*, vol. 29, no. 3, pp. 356–365, 2009.
- [10] H. Xu, H. Qian, W. Zhu et al., "Mesenchymal stem cells relieve fibrosis of *Schistosoma japonicum*-induced mouse liver injury," *Experimental Biology and Medicine*, vol. 237, no. 5, pp. 585–592, 2012.
- [11] H. Cao, W. X. H. Qian, W. Zhu et al., "Mesenchymal stem cells derived from human umbilical cord ameliorate ischemia/reperfusion-induced acute renal failure in rats," *Biotechnology Letters*, vol. 32, no. 5, pp. 725–732, 2010.

- [12] D. J. Prockop, "Marrow stromal cells as stem cells for nonhematopoietic tissues," *Science*, vol. 276, no. 5309, pp. 71–74, 1997.
- [13] D. J. Prockop, C. A. Gregory, and J. L. Spees, "One strategy for cell and gene therapy: harnessing the power of adult stem cells to repair tissues," *Proceedings of the National Academy of Sciences of the United States of America*, vol. 100, Supplement 1, pp. 11917–11923, 2003.
- [14] D. J. Prockop, "'Stemness' does not explain the repair of many tissues by mesenchymal stem/multipotent stromal cells (MSCs)," *Clinical Pharmacology & Therapeutics*, vol. 82, no. 3, pp. 241–243, 2007.
- [15] C. Thery, S. Amigorena, G. Raposo, and A. Clayton, "Isolation and characterization of exosomes from cell culture supernatants and biological fluids," in *Current Protocols in Cell Biology*, John Wiley & Sons, New York, NY, USA, 2001.
- [16] S. Lemoine, D. Thabut, C. Housset et al., "The emerging roles of microvesicles in liver diseases," *Nature Reviews Gastroenterology & Hepatology*, vol. 11, no. 6, pp. 350–361, 2014.
- [17] H. Xin, Y. Li, B. Buller et al., "Exosome-mediated transfer of miR-133b from multipotent mesenchymal stromal cells to neural cells contributes to neurite outgrowth," *Stem Cells*, vol. 30, no. 7, pp. 1556–1564, 2012.
- [18] H. C. Zhang, X. B. Liu, S. Huang et al., "Microvesicles derived from human umbilical cord mesenchymal stem cells stimulated by hypoxia promote angiogenesis both in vitro and in vivo," *Stem Cells and Development*, vol. 21, no. 18, pp. 3289–3297, 2012.
- [19] S. Gatti, S. Bruno, M. C. Deregibus et al., "Microvesicles derived from human adult mesenchymal stem cells protect against ischaemia-reperfusion-induced acute and chronic kidney injury," *Nephrology, Dialysis, Transplantation*, vol. 26, no. 5, pp. 1474–1483, 2011.
- [20] T. Li, Y. Yan, B. Wang et al., "Exosomes derived from human umbilical cord mesenchymal stem cells alleviate liver fibrosis," *Stem Cells and Development*, vol. 22, no. 6, pp. 845–854, 2013.
- [21] Y. Zhou, H. Xu, W. Xu et al., "Exosomes released by human umbilical cord mesenchymal stem cells protect against cisplatin-induced renal oxidative stress and apoptosis *in vivo* and *in vitro*," *Stem Cell Research & Therapy*, vol. 4, no. 2, p. 34, 2013.
- [22] B. Zhang, M. Wang, A. Gong et al., "HucMSC-exosome mediated-Wnt4 signaling is required for cutaneous wound healing," *Stem Cells*, vol. 33, no. 7, pp. 2158–2168, 2015.
- [23] Y. Yan, W. Jiang, Y. Tan et al., "hucMSC exosome-derived GPX1 is required for the recovery of hepatic oxidant injury," *Molecular Therapy*, vol. 25, no. 2, pp. 465–479, 2017.
- [24] S. Cui, M. Wang, and G. Fan, "Anti-HBV efficacy of bifenodate in treatment of chronic hepatitis B, a primary study," *Zhonghua Yi Xue Za Zhi*, vol. 82, no. 8, pp. 538–540, 2002.
- [25] W. Zhu, L. Huang, Y. Li et al., "Exosomes derived from human bone marrow mesenchymal stem cells promote tumor growth *in vivo*," *Cancer Letters*, vol. 315, no. 1, pp. 28–37, 2012.
- [26] T. Kawai, K. Yasuchika, T. Ishii et al., "SOX9 is a novel cancer stem cell marker surrogated by osteopontin in human hepatocellular carcinoma," *Scientific Reports*, vol. 6, no. 1, article 30489, 2016.
- [27] S. Winkler, M. Hempel, S. Bruckner, H. M. Tautenhahn, R. Kaufmann, and B. Christ, "Identification of pathways in liver repair potentially targeted by secretory proteins from human mesenchymal stem cells," *International Journal of Molecular Sciences*, vol. 17, no. 7, 2016.
- [28] Z. Zhang, H. Lin, M. Shi et al., "Human umbilical cord mesenchymal stem cells improve liver function and ascites in decompensated liver cirrhosis patients," *Journal of Gastroenterology and Hepatology*, vol. 27, no. Suppl 2, pp. 112–120, 2012.
- [29] K. Zhao, R. Lou, F. Huang et al., "Immunomodulation effects of mesenchymal stromal cells on acute graft-versus-host disease after hematopoietic stem cell transplantation," *Biology of Blood and Marrow Transplantation*, vol. 21, no. 1, pp. 97–104, 2015.
- [30] S. Zhang, L. Chen, T. Liu et al., "Human umbilical cord matrix stem cells efficiently rescue acute liver failure through paracrine effects rather than hepatic differentiation," *Tissue Engineering. Part A*, vol. 18, no. 13–14, pp. 1352–1364, 2012.
- [31] W. Zhu, L. Huang, Y. Li et al., "Mesenchymal stem cell-secreted soluble signaling molecules potentiate tumor growth," *Cell Cycle*, vol. 10, no. 18, pp. 3198–3207, 2011.
- [32] L. Sun, R. Xu, X. Sun et al., "Safety evaluation of exosomes derived from human umbilical cord mesenchymal stromal cell," *Cytotherapy*, vol. 18, no. 3, pp. 413–422, 2016.
- [33] B. Yu, X. Zhang, and X. Li, "Exosomes derived from mesenchymal stem cells," *International Journal of Molecular Sciences*, vol. 15, no. 3, pp. 4142–4157, 2014.
- [34] H. K. Seitz and F. Stickel, "Risk factors and mechanisms of hepatocarcinogenesis with special emphasis on alcohol and oxidative stress," *Biological Chemistry*, vol. 387, no. 4, pp. 349–360, 2006.
- [35] S. Dooley and P. ten Dijke, "TGF- $\beta$  in progression of liver disease," *Cell and Tissue Research*, vol. 347, no. 1, pp. 245–256, 2012.
- [36] K. Wang, "Molecular mechanisms of hepatic apoptosis," *Cell Death & Disease*, vol. 5, no. 1, article e996, 2014.
- [37] C. Y. Tan, R. C. Lai, W. Wong, Y. Y. Dan, S. K. Lim, and H. K. Ho, "Mesenchymal stem cell-derived exosomes promote hepatic regeneration in drug-induced liver injury models," *Stem Cell Research & Therapy*, vol. 5, no. 3, p. 76, 2014.
- [38] L. P. Guan, J. X. Nan, X. J. Jin et al., "Protective effects of chalcone derivatives for acute liver injury in mice," *Archives of Pharmacological Research*, vol. 28, no. 1, pp. 81–86, 2005.
- [39] S. Y. Gui, W. Wei, L. W. H. Wang, W. Y. Sun, and C. Y. Wu, "Protective effect of *fufanghuangqiduogan* against acute liver injury in mice," *World Journal of Gastroenterology*, vol. 11, no. 19, pp. 2984–2989, 2005.